Pulsar PSR B2303+30: a single system of drifting subpulses, moding and nulling

Stephen L. Redman,[1]⋆ Geoffrey A. E. Wright[1,2]⋆ and Joanna M. Rankin[1]⋆

[1]*Physics Department, University of Vermont, Burlington, VT 05405, USA*
[2]*Astronomy Centre, University of Sussex, Falmer, Brighton BN1 9QJ*

ABSTRACT

Analyses of multiple pulse sequences of the pulsar PSR B2303+30 reveal two distinct emission modes. One mode (B) follows a steady even–odd pattern and is more intense. The second mode (Q) is characteristically weak, but has intermittent drift bands with a periodicity of approximately $3P_1$/cycle, and nulls much more frequently than the B mode. Both modes occur with roughly equal frequency, and their profiles have a similar single-humped form with a slight asymmetry. Our observations and analyses strongly suggest that the subpulse drift rates in both modes are linked in a series of cycles, which can be modelled as relaxing oscillations in the underlying circulation rate.

Key words: MHD – plasmas – polarization – radiation mechanisms: non-thermal – pulsars: general – pulsars: individual: B2303+30.

1 INTRODUCTION

The phenomena of drifting, moding and nulling are not new concepts to the pulsar community. However, rarely has a pulsar offered such insight into its own inner workings through the interaction of these three phenomena. Not only does PSR B2303+30 provide us with numerous examples of drifting subpulses, moding and nulling, but also it offers enough clues to model its behaviour empirically, as a single system.

PSR B2303+30 is an old, bright pulsar with a relatively long rotation period (P_1) of 1.57 s. Since its discovery (Lang 1969), it has been the subject of a number of studies, which have emphasized measurements of P_2, the longitudinal distance between adjacent subpulses, and P_3, the number of rotation periods that elapse before the subpulses return to their original phase (Taylor & Huguenin 1971; Backer 1973; Sieber & Oster 1975). It is one of seven well-known pulsars with a clear even–odd modulation: of which B0943+10 is also a prominent member, the others being B0834+06, B1633+24, B1933+16, B2020+28 and B2310+42 (Oster, Hilton & Sieber 1977; Wolszczan 1980; Rankin 1986; Hankins & Wolszczan 1987). Careful analyses of B0943+10 have led to the delineation of its rotating sub-beam configuration (Deshpande & Rankin 1999, 2001). Given the similarities between B0943+10 and B2303+30, it seems reasonable to assume that similar analyses might reveal greater details concerning the drift behaviour of B2303+30. However, the drift behaviour of B2303+30 is much more complicated than that of B0943+10. The brightest drifting subpulses of B2303+30 do not often have a single steady

⋆E-mail: stephen.redman@uvm.edu (SLR); gae@sussex.ac.uk (GAEW); joanna.rankin@uvm.edu (JMR)

drift rate, but instead appear to oscillate about $P_3 \approx 2$ periods/cycle (hereafter P_1/cycle or P_1/c). Various models have been applied to this strange feature (Gil, Hankins & Nowakowski 1992; Gil & Sendyk 2000) – however, we are confident that our latest analyses provide sufficient reasons for advancing a more comprehensive explanation.

A glance at a typical B2303+30 sequence will confirm without a doubt that it exhibits a strong even–odd modulation ($P_3 \approx 2P_1$/c) with considerable variation (see Fig. 1 for three sample total-power sequences). In addition to the clear even–odd modulation, there is a second behaviour, which, when viewed under good signal-to-noise ratio (S/N) conditions, occasionally reveals a steady $P_3 \approx 3P_1$/c. Because such intervals are characterized by frequent nulls and sometimes erratic behaviour, they were difficult to discern in older observations. This change in behaviour is quasi-periodic, suggesting that regular events in the pulsar's magnetosphere or on the crust of the neutron star disturb the drift. Because these behaviour changes are so frequent, B2303+30 presents us with a unique opportunity to use mode changes as a method for modelling the drifting subpulse behaviour.

We therefore argue that there are in principle two modes in B2303+30, which can be identified based on their modulation patterns and total-power intensities. The first, which we call the 'B' (burst) mode, has a modulation pattern with a P_3 very close to $2P_1$/c and is relatively luminous compared to the second mode, which we call the 'Q' (quiescent) mode. The Q-mode pattern has a P_3 close to $3P_1$/c, is dimmer than the B mode, and also nulls much more frequently. These specific modulation patterns are possible only under certain alias conditions, which allow us to posit a basic model of the sub-beam rotation. This model unites the basic features of drifting, moding and nulling as a single cyclic system.

Table 1. Observations.

Date	Frequency (MHz)	Pulses	Bandwidth (MHz/#Ch[a])
1992 October 15	430	2370	10/32
1992 October 18	1414	1470	20/32
1992 October 19	1414	1008	20/32
2003 July 17	1525	2815	100/32
2003 October 7	327	1525	25/256
2003 October 20	327	1523	25/256

[a]Number of channels.

After providing the details of our observational methods in Section 2, we describe our basic method of behavioural analysis in Section 3, in which we suggest that the two behaviours represent two distinct emission modes in B2303+30. Null analyses of the two modes are covered in Section 4, followed by the deduced geometry of B2303+30 in Section 5 and our drifting sub-beam model in Section 6. In Section 7, we discuss how these implications relate to magnetospheric theories. Finally, in Section 8, we review our conclusions.

2 OBSERVATIONS

The analyses in this paper are based on six observations, all of which were carried out at the Arecibo Observatory (AO) in Puerto Rico over the past 12 yr as described in Table 1. These measured the four Stokes parameters, I, Q, U and V, of the pulse sequences at various frequencies and to varying degrees of accuracy. The 1992 sequences were recorded at 430 or 1414 MHz using the then existing Arecibo 40-MHz Correlator, and details of the polarimetry and calibration can be found in Hankins & Rankin (2004, hereafter HR). The 2003 observations were acquired with the Arecibo Wide Band Pulsar Processor (WAPP[1]) using either 256 channels across a 25-MHz passband at 327 MHz, or 64 channels within a 100-MHz bandwidth at 1525 MHz. In both series the measured auto- and cross-correlation functions were corrected for sampling errors, differential instrumental phase, Faraday rotation across the passband and parallactic angle. The earlier observations are also corrected for instrumental cross-coupling, but this further correction was not yet available for the 2003 data – and in any case would be slight owing both to the quality of the feeds and to the pulsar's modest levels of fractional linear polarization.

The 1992 observations have a resolution of 0.275° longitude, the first two 2003 observations have a resolution of 0.352° longitude, and the 2003 October 20 observation has a resolution of 0.468° longitude.

3 THE TWO EMISSION MODES

Fig. 1 shows three different 200-pulse total-power sequences. The left and centre plots are from a 430-MHz observation. The plot on the right is from the 327-MHz observation. These same three pulse sequences (PSs) can be seen in Fig. 2, where only the odd pulses are plotted, at double height. With these displays, the apparent direction and speed of the drifting subpulses become much clearer.

In the first 430-MHz PS, we see an unusually long B-mode interval (pulses 1–170). Note the steady even–odd modulation that appears to drift towards the leading edge of the profile, especially
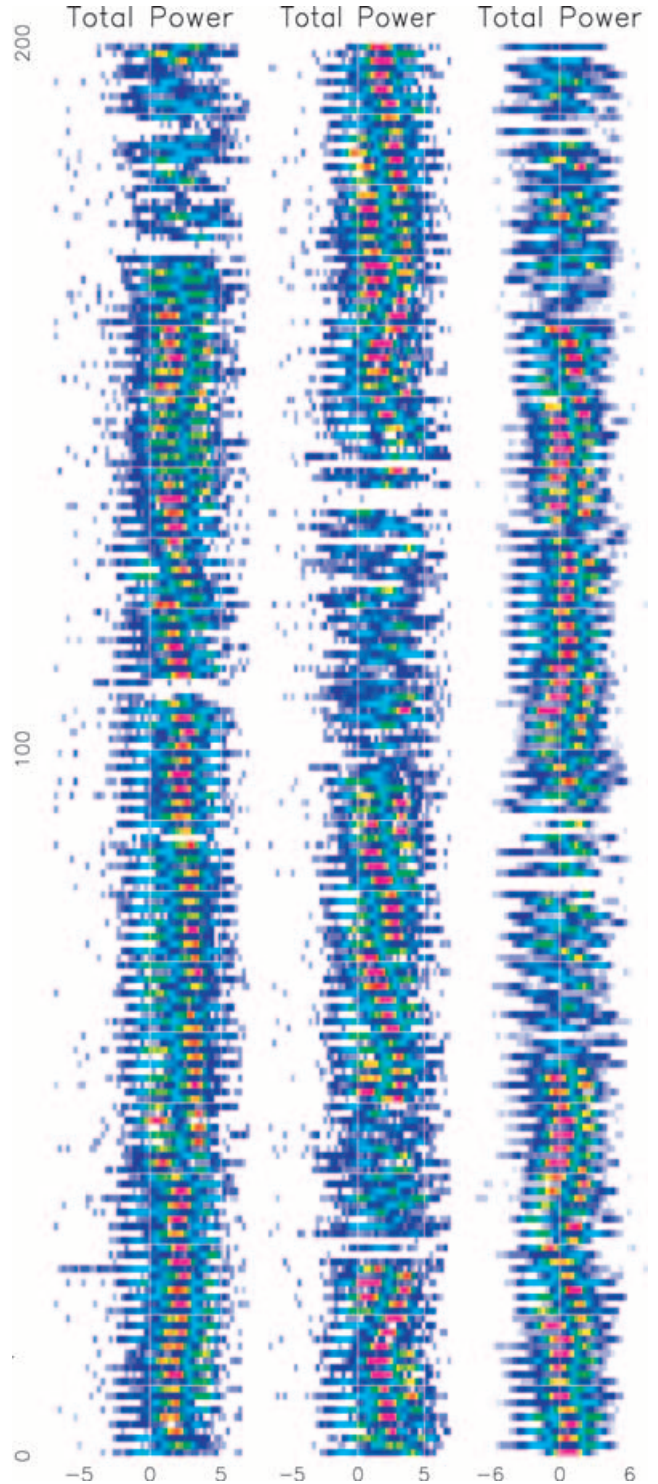

Figure 1. Three different 200-pulse, total-power sequences of B2303+30, where pulse number is plotted against the longitude in degrees via a colour scale where blue increases to green and then to red. The left and centre plots are from the 430-MHz observation, and the plot on the right is the 2003 October 7 observation at 327 MHz. Note the exceptionally long B-mode sequence ($P_3 \approx 2P_1$/c) in the left-hand panel, the varying P_3 of the B-mode sequences in the centre panel, and the Q-mode intervals ($P_3 \approx 3P_1$/c) that interrupt the B mode in the right-hand panel.
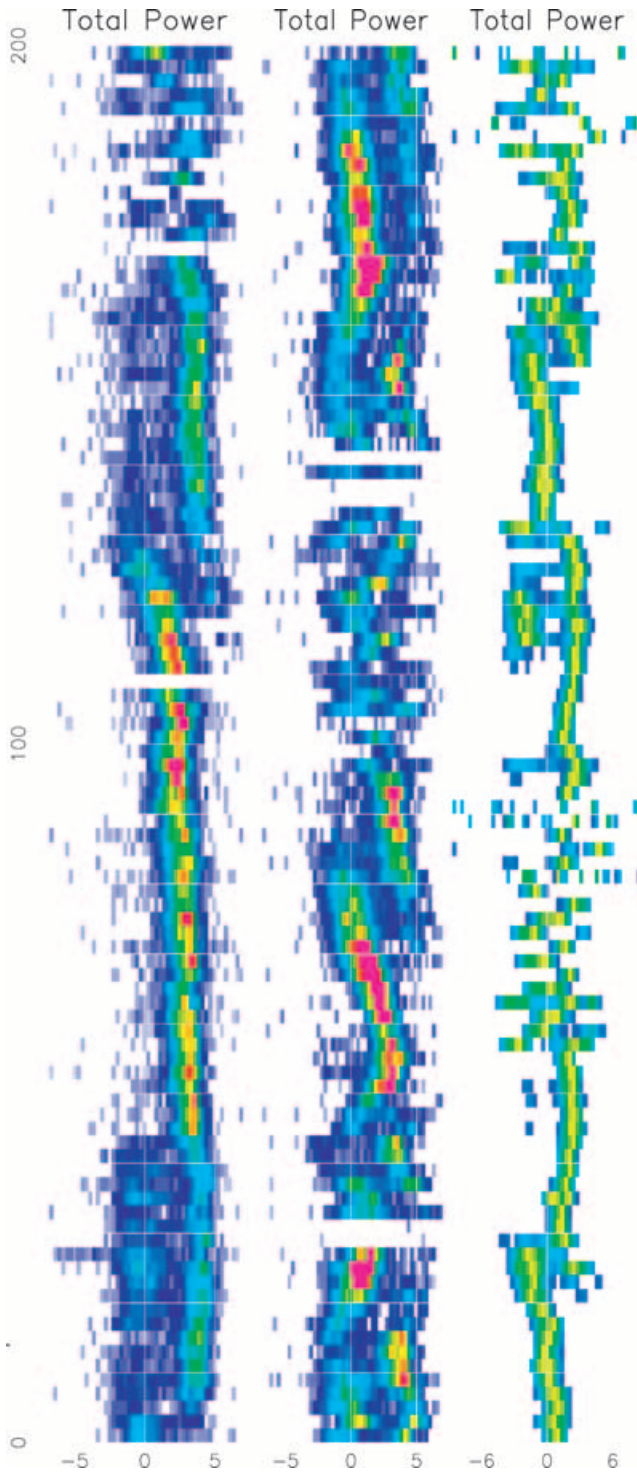
Figure 2. The same three 200-pulse, total-power sequences seen in Fig. 1, but with only the odd pulses, plotted at double height. The plot on the far right, at 327 MHz, is normalized so that all pulse peaks appear the same colour. In these plots, the B-mode drift appears steady, while the Q mode appears disordered. Notice that there appear to be at least two different kinds of B-mode behaviour: one in which the modulation is exactly $2P_1/c$ (as between pulses 1–39 in the left-hand panel), and another where the B-mode appears to oscillate around (but not at) $2P_1/c$ (as between pulses 143–197 of the centre panel).
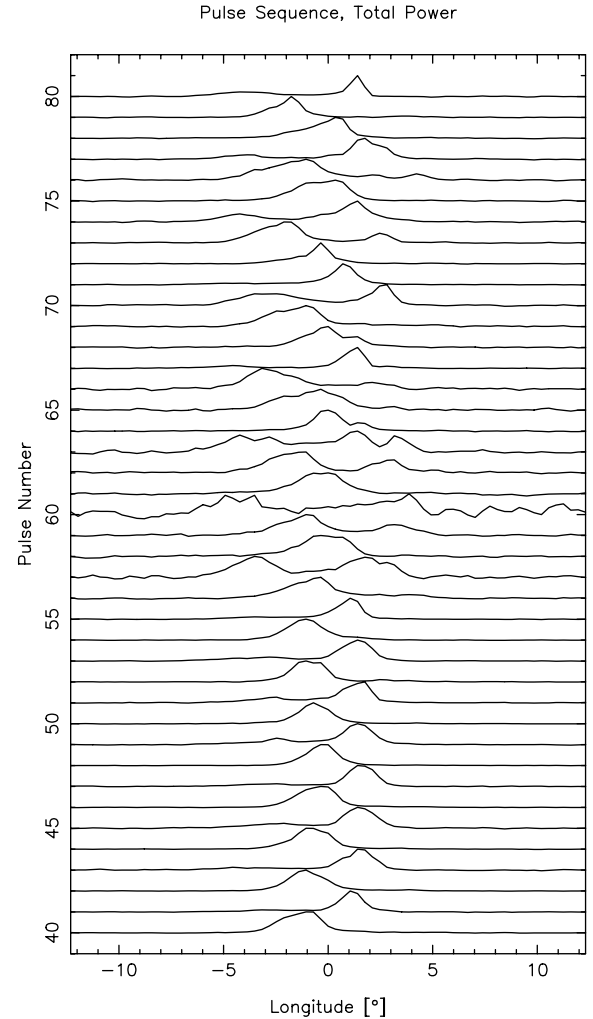

Figure 3. Pulses 40–80 of the 327-MHz observation (2003 October 7, also seen in the right-hand panel of Fig. 1), normalized so that all pulses peak at the same height. The two modes can be identified by their respective drift rates. Pulses through number 56 or 57 are B mode, and the Q mode finishes the sequence. Pulse 60 is not a null, but a weak pulse.

near pulse 170. After two nulls, this even–odd modulation switches to an apparently chaotic behaviour with no obvious drift direction. This is the behaviour noted by Rankin, Campbell & Backer (1974) and Gil et al. (1992).

In the middle sequence (also at 430 MHz), the B mode is much less steady, changing apparent drift direction frequently. The short drift towards the right (pulses 33–41) has a P_3 with the characteristic B value of $\approx 2P_1/c$, but is relatively weak. There are also two examples of what appears to be an 'oscillation' of P_3 (between pulses 33–95 and 143–197). It is this slight variation in P_3 which Gil et al. (1992) identified as a second B mode. This variation in P_3 often occurs immediately after a transition to the B mode. Between the two B-mode sequences, another chaotic PS appears.

In the 327-MHz sequence, the larger S/N makes the drift behaviour of the seemingly chaotic intervals much more apparent than in former observations. The B mode begins the sequence, then switches to a steady $P_3 \approx 3P_1/c$ PS around pulse 57. This transition can be seen in greater detail in Fig. 3. Notice that the transition between behaviours is smooth and unbroken. This second behaviour continues through several nulls until pulse 92, where the pulsar returns to B mode, only to switch back after pulse 160.

It is our conclusion that these 'chaotic' sequences represent a second mode, the 'Q' mode. While this second behaviour appeared completely disordered in earlier data, more recent observations reveal that it frequently has a quasi-steady $P_3 \approx 3P_1$/c. However, the Q mode also exhibits numerous nulls and can otherwise appear disordered.

We also note an intriguing subpulse pattern that sometimes follows a strong B-mode sequence. Here a drift again close to $P_3 \approx 3P_1$/c is discernible, but counter in sense to Q (i.e. drifting from leading to trailing edge). Such sequences, which we call the Q* mode because of its 'conjugate' nature, are infrequent (a clear example does not appear in Figs 1 and 2, but a few can be seen later in Fig. 17), but none the less are found in all data that possess strong S/N, and we argue in Section 6 that they are powerful clues to the underlying subpulse behaviour.

A further point should be noted here: nulls frequently occur at the transition boundaries between modes, although transitions from the B to the Q mode are also sometimes surprisingly smooth (Fig. 3). This distinction will become significant later when we attempt to model the drift behaviour.

3.1 Mode identification and statistics

After displaying and studying each PS, we attempted to identify the mode of each pulse. PSs were categorized as either B- or Q-mode pulses based upon the P_3 of the sequence (B mode: $P_3 \approx 2$; Q mode: $P_3 \approx 3$ or confused). This procedure was carried out entirely by eye, using coloured displays such as those seen in Figs 1 and 2.

This could not, admittedly, be accomplished without some subjectivity. For example, in Fig. 3 a smooth transition from the B to the Q mode can be seen at pulse 57. Do we classify pulse 57 as a B- or a Q-mode pulse? Or, if a null occurs between modes, as it often does, do we classify the null as belonging to the B or the Q mode? Clearly, for some analyses, such as constructing partial modal profiles, a decision such as this would make little difference. However, the issue becomes more complicated if, for example, we classify all transition nulls as belonging to the Q mode and then later conclude that the Q mode nulls more frequently than the B mode. For the purpose of such accounting then, the transition pulses (or nulls) were simply ignored.

The occurrence frequency of the two modes is consistent among the available observations. Some 45.7 and 54.3 ±1 per cent of the 9188 pulses we observed are Q-mode and B-mode pulses, respectively. The average length of a B-mode sequence is 37 pulses, and that of a Q-mode 31 pulses.

Fig. 4 shows a histogram of B- and Q-mode lengths. Notice that the B mode sometimes persists for very long stretches, some of which are well over 100 periods – but the Q mode never seems to last for more than about 70 pulses. Note also that both B and Q distributions exhibit short (i.e. typically $10P_1$) as well as long (typically 30–$40P_1$) sequences.

It is interesting to explore the origin of these features. If we consider the sequence of pulses 97–140 in the centre panel of Fig. 1, we might be tempted to classify the entire sequence as Q mode. However, closer inspection suggests that a short sequence of B occurs from pulses 103–107 (because of its on–off character and slightly greater intensity). This then results in the recording of two medium-length Q-mode (97–102 and 108–140) and a short B-mode sequence in our statistics. However, had the quality of our data been lower (through scintillation effects, which varied during some of our observations) this Q–B–Q transition might have gone undetected. This implies that in the overall emission behaviour of this pulsar
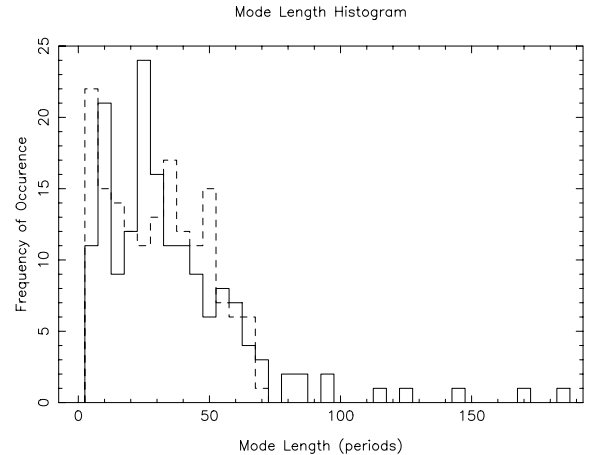

Figure 4. Mode lengths, from all observations: B mode is shown solid, and Q mode is dashed. Notice that the B mode can last for over 100 periods, but no Q-mode PS longer than 71 periods was observed. Note also the apparent excess of short modes in both distributions.

we are seeing B-mode stretches of 30–40 periods interspersed by Q-mode stretches of similar duration, which at least on some occasions contain intermittent brief ($<10P_1$) B-mode sequences. Although we tried hard to avoid it, short B- and Q-mode sequences in Fig. 4 are very likely under-accounted and long Q-mode sequences over-accounted. These are the basic features on which we seek to shed light in our discussion in Section 6.

3.2 Integrated profiles

Partial total-power profiles, comprising pulses identified as belonging to the B and Q modes, were first computed so that their relative average intensity might be compared, and then scaled so that the profiles had the same height. The scaled profiles allowed us to compare the shapes of each modal partial profile. Figs 5 and 6, at 430 and 1525 MHz, respectively, each show a relative and scaled profile of B2303+30.
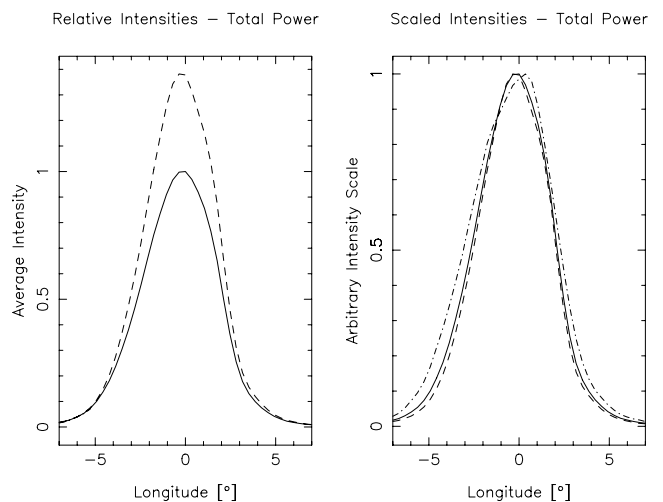

Figure 5. B-mode (dashed), total (solid) and Q-mode (dash-dotted) total-power profiles at 327 MHz (2003 October 7 observation). The average profile peak of the Q mode is about 43 per cent that of the B-mode between 0.3 and 1.6 GHz. The figure on the right shows the same profiles, all scaled to the same arbitrary height. Notice that the Q-mode profile is noticeably wider than its B-mode counterpart.
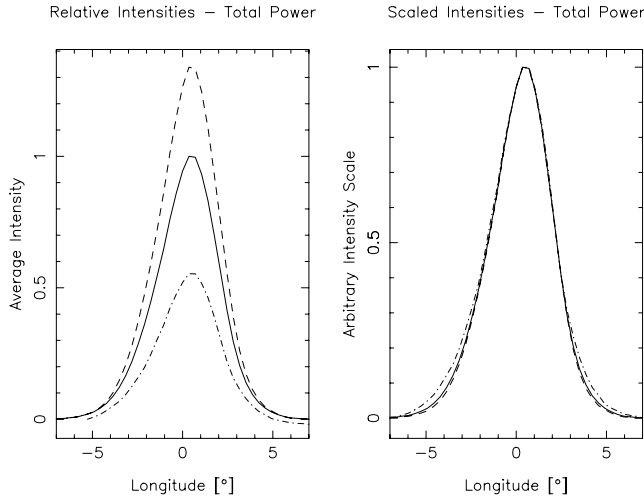
Relative Intensities − Total Power   Scaled Intensities − Total Power

Figure 6. Total-power profiles as in Fig. 5 at 1525 MHz. Again, note that the Q-mode is both weaker and slightly wider than the B-mode profile.

In both figures, two circumstances can be easily confirmed. First, the B mode is significantly brighter than the Q mode. Among the six observations, the B mode was, on average, 2.32 ± 0.31 times as intense as the Q mode. Secondly, the Q-mode profile is noticeably wider than its B-mode counterpart. The causes of this half-width increase are, at this point, not well understood. However, it can be seen that this increase is less pronounced at the higher frequency. It should also be noted that B2303+30 has a slightly asymmetric average profile – the trailing edge is slightly steeper than the leading edge of the profile. Information about the polarization–modal structure of the profiles of B2303+30 can be found in Ramachandran et al. (2002), as well as in Rankin & Ramachandran (2003) and HR.

3.3 Intensity variations

Having discovered how dramatically different the average intensities of the modes are, we now examine the long-term intensity variations. Fig. 7 gives the relative integrated intensity of a 2000-pulse sequence at 430 MHz. The clear and quasi-periodic variations in intensity are not the result of scintillation; it is a feature of B2303+30 that is seen at all observed frequencies. As might be expected from the previous subsection, these variations in integrated intensity result from the fact that the pulsar has two modes, each with a characteristic intensity.

The mode-dependent intensity variations are even more clearly demonstrated when normalized PSs are compared with the integrated intensity of the same sequence. Fig. 8 shows the same 40-pulse sequence seen in Fig. 3. Notice that there is a pronounced intensity decrease around pulse 57 in Fig. 8, corresponding exactly to the change in P_3 shown in Fig. 3. Thus, these changes in intensity are characteristic of each mode.

These changes in intensity also represent a second method of identifying the modes. This method is less reliable than distinguishing between the modes using P_3, however, and thus was only used to clarify a possible mode change.

3.4 Subpulse modulation

As indicated at the beginning of Section 3, the two modes each exhibit a unique but varying P_3. The longitude-resolved fluctuation
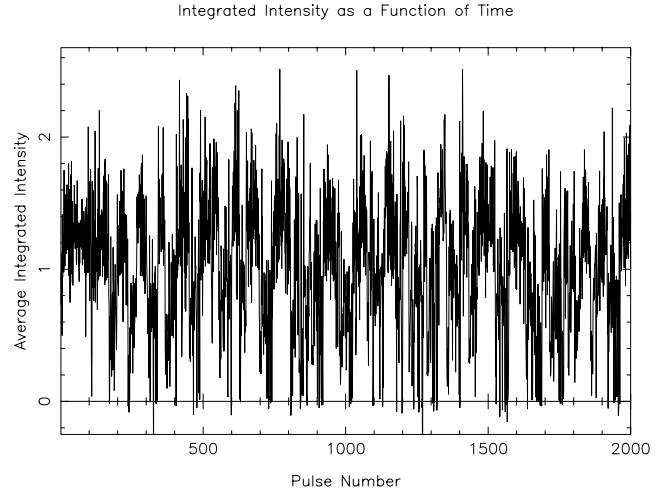
Integrated Intensity as a Function of Time

Figure 7. The average integrated intensity of a sequence of single pulses at 430 MHz. Note the pronounced intensity 'states' of the brighter B and weaker Q modes – in roughly a ratio of 2 : 1. One can even clearly pick out the exceptionally long B-mode PS that begins this observation. Note also how the B and Q modes alternate with a quasi-regular periodicity.
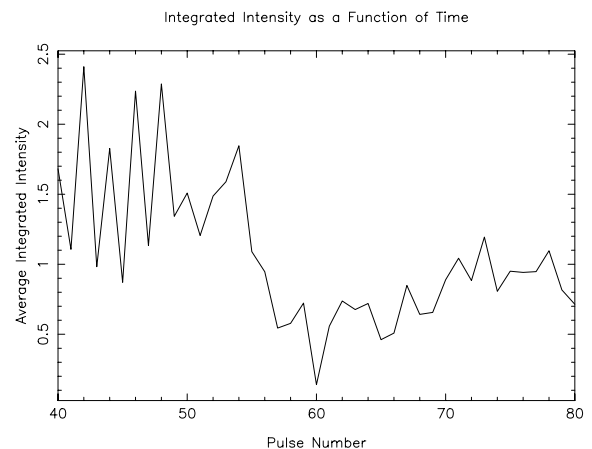
Integrated Intensity as a Function of Time

Figure 8. Intensities of the same 40-pulse interval seen in Fig. 3. Here the two modes can be identified by their respective total intensities. Notice the clear drop in intensity around pulse 57, coinciding with the change in drift rate seen in Fig. 3.

(LRF) spectra of all 2370 pulses at 430 MHz (see Fig. 9) reveals the complexity of the subpulse modulation of B2303+30. Strong features are visible in several locations throughout the integral spectrum (bottom panel). The origin of these features will be discussed below.

From the LRF spectra, it is impossible to determine whether the features are indicative of the pulsar's true frequencies and drift directions, or aliases thereof. Additional information can be obtained, however, by computing a harmonically resolved fluctuation (HRF) spectrum. The HRF spectrum is calculated by overlapping fast Fourier transforms (FFTs) of length 256 and then interpolating between adjacent Fourier amplitudes to estimate the frequency of the feature and its errors (for further details see Deshpande & Rankin 2001). Furthermore, HRF spectra can sometimes distinguish between amplitude and phase modulations. Amplitude modulations appear as symmetric feature pairs in the integral spectrum, whereas phase modulations are asymmetric. The beautiful HRF spectrum of
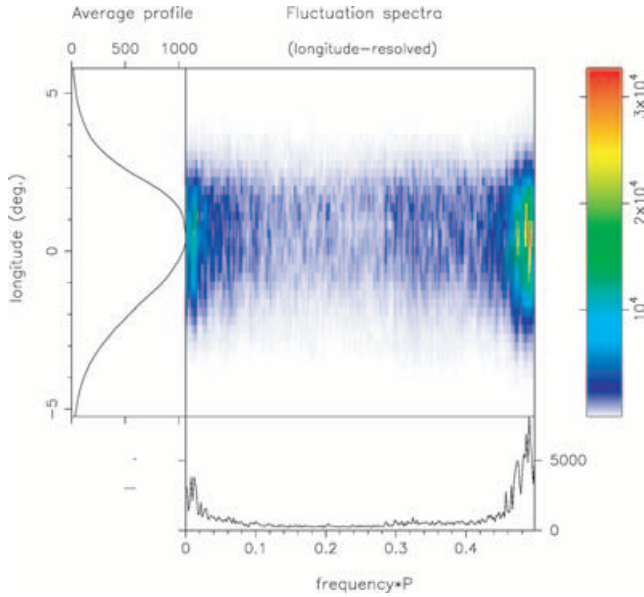
Figure 9. Longitude-resolved fluctuation spectra for pulsar B2303+30 at 430 MHz. A 512-point FFT was used and averaged over all 2370 pulses of the 1992 October 15 observation. The body of the figure gives the amplitude of the features, according to the colour scheme on the right. The average profile (Stokes parameter I) is plotted in the left-hand panel, and the integral spectrum is given at the bottom of the figure. Note the numerous features, particularly those around 0.01, between 0.29 and 0.45, and between 0.45 and 0.49 c/P_1, as well as the asymmetry of the profile, briefly noted in Section 3.2.

the entire 430-MHz sequence, computed with an FFT of 256 points, can be seen in Fig. 10.

To determine the sources of these features, a simple pulsar model was computed, complete with strong B-mode ($P_3 \approx 2P_1$/c) and weak Q-mode ($P_3 \approx -3P_1$/c) emission, each with moderate variation in their P_3 values. The Q* mode ($P_3 \approx 3P_1$/c) was not included in this model because the Q* mode in the observational HRF is both infrequent and weak. This model pulsar had an average profile with a half-power width of 6°, intensity variations (B-mode subpulses are 2.3 times as amplified as Q-mode subpulses) and mode durations that ranged between 29 and 71 periods. Neither nulls nor noise were included in the simulation. The resulting HRF of the simulation can be see in Fig. 11. Notice that the four features mentioned above appear here in decent detail. By altering and eliminating certain variables (such as the length of the modes, or the intensity of the emission), we could discern the source of those features seen in Fig. 10.

The first is that seen near 0.5 c/P_1. This feature is due primarily to the B-mode modulation. Notice, though, that this feature is not smooth, but comprises high-Q ($=f/\Delta f$) 'spikes' – produced both by the variety of semi-discrete P_3 values the B-mode exhibits, as well as by the fact that there are two prominent P_3 values in this pulsar, the combination of which produces periodic 'beats' in the frequency spectrum.

The second of the four prominent features in Fig. 10 falls between 0.28 and 0.44 c/P_1. This feature, which is also prominent in the body of the figure, is produced by Q-mode emission, as well as the above-mentioned 'beat' phenomenon. Notice that this feature is not reflected about 0.50 c/P_1, and thus represents phase modulation. The simulation verifies that the above feature reflects a specific drift direction (i.e. negative). What is of great significance is the
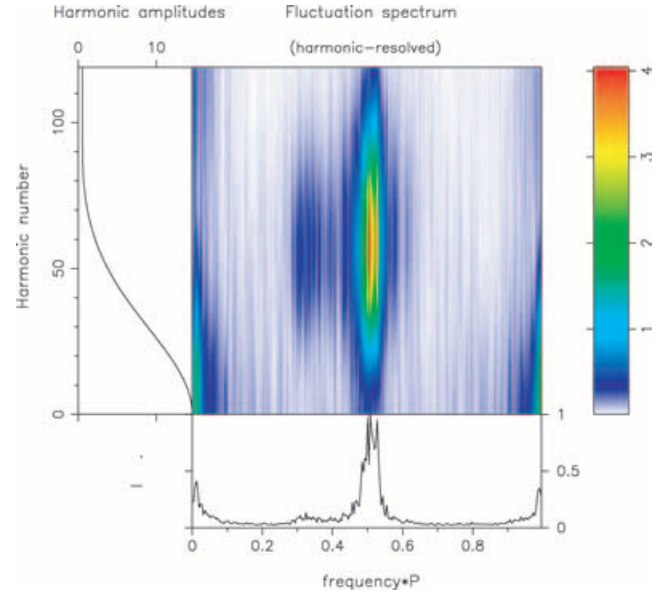

Figure 10. A harmonically resolved fluctuation spectrum of all 2370 pulses in the 430-MHz observation from 1992 October 15. The left-hand panel gives the amplitude of frequency components at integral multiples of the pulsar rotation frequency, 1/P_1. The body of the figure then gives the amplitude of all the other frequency components in the spectrum up to 120/P_1 according to the colour scheme at the right. The bottom panel shows the sum of these frequency components, collapsed on to a 1/P_1 interval. The features now fall at their true (partially unaliased) frequency. The B-mode features can be seen around 0.5 c/P_1, corresponding to a $P_3 \approx 2P_1$/c. The Q-mode feature, with a $P_3 \approx 3P_1$/c, can be seen to the left of the B-mode feature. There are also two other features to be considered in this diagram – one close to 0.01 c/P_1, and a second near 0.99 c/P_1 – which represent an amplitude modulation that occurs every 80 pulses or so, the approximate sum of a given B- and Q-mode pair. This amplitude modulation is apparent in Fig. 7.

appearance in Fig. 11 of a wide range of beat features surrounding both the basic B-mode and Q-mode frequencies. Although in the natural pulse sequences a significant 'jitter' is undoubtedly present in both, many of the broad frequency features surrounding $P_3 = 0.33$ and 0.5 visible in Fig. 10 may be due to the beat phenomena.

The third and fourth features in Fig. 10 are reflections of each other – one at 0.012 c/P_1 and the other at 0.988 c/P_1 – corresponding to an amplitude modulation of about 90 ± 10 P_1/c. These features are due to the amplitude modulation that occurs between successive B- and Q-mode PSs (e.g. Figs 4 and 7).

4 NULLS

As can be seen in the three PSs of Fig. 1, B2303+30 occasionally emits at such low intensity that the pulsar appears to null. These low-intensity intervals appear to be much more frequent during Q-mode intervals, but a few can be found within B-mode sequences as well. Transition intervals of low intensity between modes also occur throughout the PSs, as can be seen, for example, in the left-most panel of Fig. 1.

4.1 Nulls or weak pulses?

To determine whether these low-intensity intervals are nulls or simply low-intensity pulses, we computed a histogram of the average pulse intensity. Fig. 12 shows this histogram, segregated by modes. For reasons discussed in Section 3.1, 126 transition pulses have been
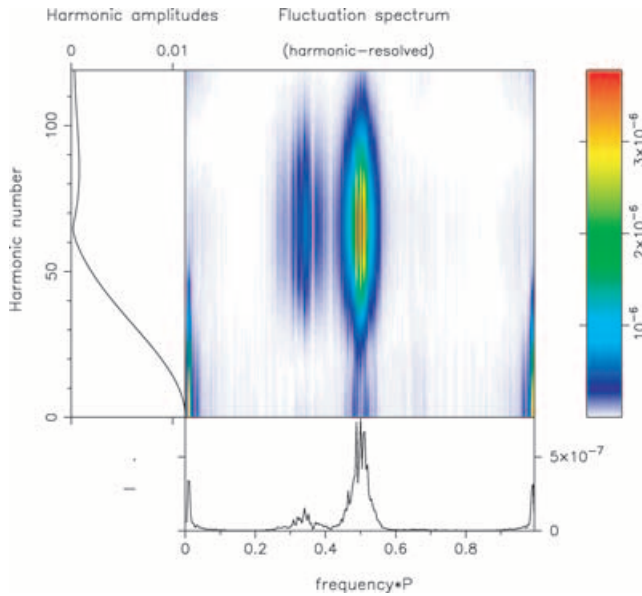
Figure 11. A harmonically resolved fluctuation spectrum of 1000 simulated pulses. Notice the similarity of features seen in Fig. 10, such as the strong B-mode feature, the weaker Q-mode feature, and a strong amplitude modulation at either end of the frequency spectrum.

excluded from this analysis. Pulses that occur at or very near zero average integrated intensity – that is, that are indistinguishable from the noise distribution – are considered nulls. From this figure, we can see that the B mode lacks any definite nulls. The Q mode shows two distinct populations of nulls and pulses, but there is a slight overlap between the two near 0.15 times the average intensity. This strongly suggests that B2303+30 does indeed null, and predominantly (if not entirely) in one mode.

Fig. 12 provides us with a definition for null pulses. Those pulses with an average on-pulse integrated intensity below 12 per cent of the average integrated intensity were considered nulls. This integrated
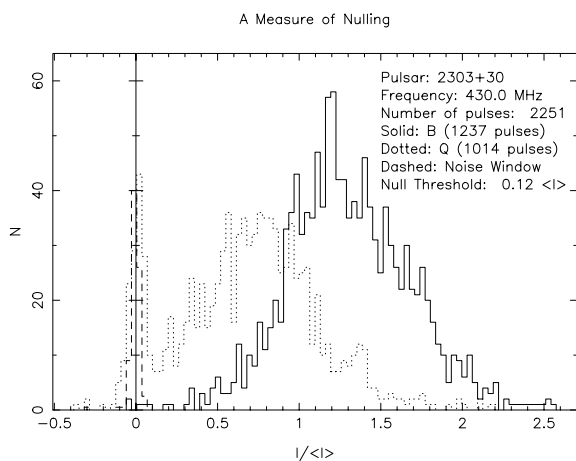

Figure 12. Null-frequency histogram for the B (solid) and Q (dotted) modes. Transition pulses have been ignored for reasons discussed in Section 3.1. Notice that the small population of B-mode nulls is well separated from the B-mode pulses, but that the Q-mode pulse and null distributions overlap slightly. Also note that the Q-mode nulls have a distribution very similar to the off-pulse noise (dashed), which has been calculated from an equal number of samples from the off-pulse window of the Q-mode nulls, then reduced in height by a factor of 2.

Table 2. Null statistics.

Pulse population	Frequency of occurrence (per cent)	Maximum (periods)	Average (periods)
All pulses	10.02 ± 1.67	11	1.84 ± 0.20
B mode	0.45 ± 0.30	2	1.14 ± 0.46
Q mode	20.03 ± 2.44	8	1.84 ± 0.32
Transition	17.11 ± 5.71	11	1.51 ± 0.51

intensity minimum occurred in all of the observations, and thus provided a consistent definition of a null. To confirm that these pulses were actually nulls, we created average profiles of null pulses (including transition nulls) at different frequencies. These profiles (not pictured) revealed that there was no significant power in those pulses that were considered nulls.

4.2 Null statistics

Table 2 confirms what Fig. 12 suggests – that the Q mode nulls much more frequently than the B mode. Note that, since nulls are defined as pulses below a specific integrated intensity level, these null distributions include weak pulses that fall below this level. The errors listed in this table are one standard deviation.

Transition nulls are nulls that occur between modes, and thus could not be categorized beforehand as belonging to the B or Q modes. The low occurrence frequency of B-mode nulls (if any) and the relatively large frequency of Q-mode nulls suggest that those nulls which belong to transition pulses are in fact Q-mode nulls. This conclusion is further reinforced by the fact that the null distributions of the Q mode and of the transition pulses overlap. Indeed, given the inherent difficulty in assigning a null to a particular mode, our results are consistent with the statement that the B-mode *never* nulls. This is the first pulsar where the null fractions are strongly mode-dependent.

Fig. 13 shows a histogram of null lengths. Longer nulls are relatively infrequent compared with short nulls. This suggests that very short nulls – nulls less than one period – probably occur.
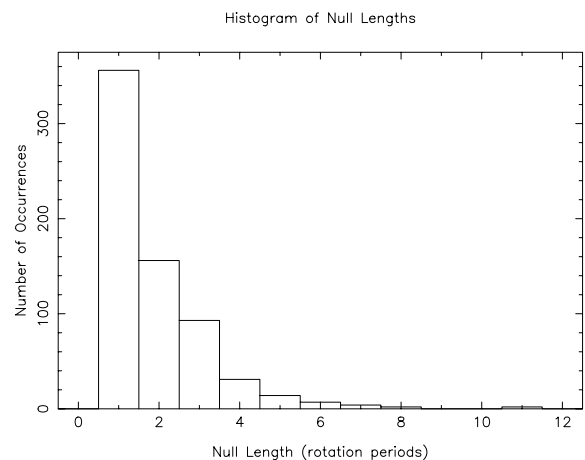

Figure 13. A histogram of null lengths from all available PSs. Notice that longer nulls are less frequent, indicating that very short nulls (nulls less than one period) probably exist.
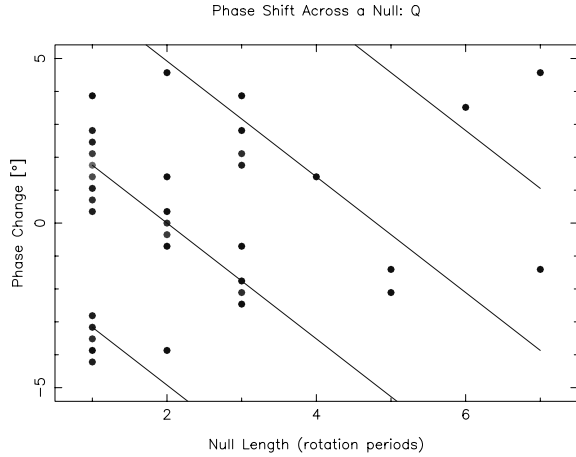
Figure 14. Phase change of subpulse peak across Q-mode nulls at 327 MHz (2003 October 7). The solid lines represent drift with a $P_3 = 3$. Since the phase change across a null appears to be dependent upon the length of that null, B2303+30 has memory.

4.3 Subpulse memory

When subpulse drift appears to be continuous across a null, the pulsar is said to exhibit 'memory'. The existence of this quality is established by examining the peak phase of individual pulses before and after a sequence of nulls. If the pulses have a constant phase change of about $0°$ across any number of nulls, the pulsar does not have memory. Likewise, if the phase change of the pulses shows a linear increase or decrease, drifting continues across nulls, and the pulsar is said to have memory.

Fig. 14 shows a plot of phase change versus Q-mode null length at 327 MHz (2003 October 7 observation). B-mode nulls have been excluded because they exhibit a different drift rate, and transition nulls have been excluded because they have no consistent drift rate. Notice that the points appear to follow lines of near-constant Q-mode drift, suggesting that B2303+30 does indeed have memory.

5 GEOMETRY AND 'ABSORPTION'

A crucial question in the analysis of any pulsar exhibiting subpulse drift is its emission geometry – that is, its magnetic inclination angle α and sightline impact angle β. An early attempt to determine these values was made by one of us (Rankin 1993a,b) using a polarization-angle (PA) sweep rate of 4.5 deg/deg (Lyne & Manchester 1988), resulting in α and β values of 20.5 and $4.5°$, respectively. Unfortunately, we now have confirmed from several directions that such PA sweep-rate determinations are particularly difficult for the conal single (S_d) stars most closely associated with subpulse drifting, because of polarization-mode mixing on the edges of the conal beam (Ramachandran et al. 2002; Rankin & Ramachandran 2003; Ramachandran et al. 2004). Indeed, the PA histogram in the 2002 paper indicates a sweep rate near 8.5 deg/deg, which has now been confirmed by recent AO observations in this paper (not shown; see also HR). Keeping the assumption of an outer cone, α would then be some $40°$ without much change in β.

However, this is not the only issue: (a) not only do we lack any strong evidence (low-frequency profile bifurcation) that the pulsar has an outer cone, the near-invariance of its profile (HR) might suggest an inner one; and (b) every well-studied S_d star so far has been found to exhibit some profile 'absorption', so we cannot be sure that the single profile we observe represents a full traverse through
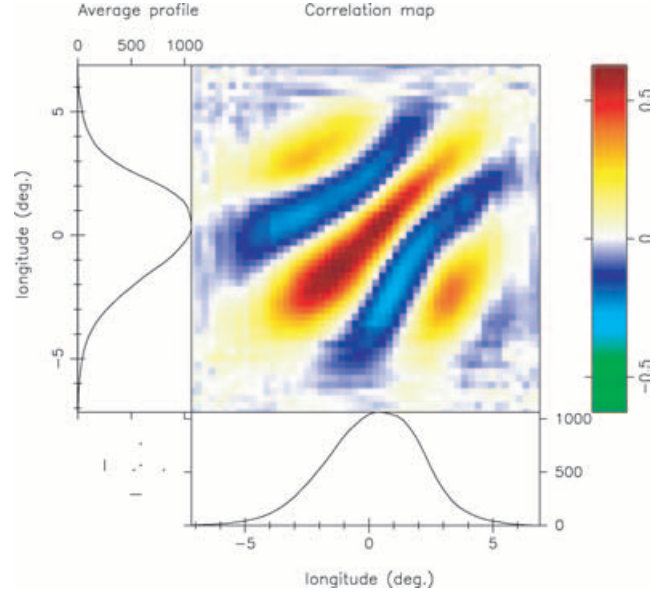

Figure 15. Beautiful evidence that the metre-wavelength profile of B2303+30 is not complete. The figure gives a colour–intensity coded longitude–longitude correlation plot at a lag of 2. Notice that the correlation is not symmetrical about the peak of this 430-MHz PS profile (plotted in both the left-hand and bottom panels). The symmetry point rather falls near its trailing half-power point. The vertical or horizontal interval between the maxima is also a measure of the subpulse separation P_2. See text for more details.

its emission cone. Indeed, the asymmetry of its profile in both total power and modal polarization also suggests that the profile of B2303+30 is incomplete on the trailing side, and the longitude–longitude correlation plot in Fig. 15 comes close to proving this circumstance. None the less, were its full profile even twice as wide (9–$10°$), corresponding to the magnetic-axis longitude falling at about the half-power point on the trailing profile edge, α could not be as small as $20°$.

Difficult observations at 100 MHz and below are needed to resolve the geometry of B2303+30. The 102-MHz observations (Malofeev, Izvekova & Shitov 1989; Suleymanova, private communication) suggest an unresolved double form, and certain 111.5-MHz AO profiles from the same era confirm this suggestion (HR); however, we know of no observation of adequate quality that exists to fully resolve whether or not the star's profile bifurcates in the expected outer cone manner.

Consequently, on the available evidence above we can reasonably guess that the star has an inner cone and a nearly constant profile half-power width of some $9.5°$ such that only the leading part is seen at metre wavelengths and higher. The second 'component' at 100 MHz then corresponds to that 'absorbed' at higher frequencies. Recomputing the geometry using the above PA sweep-rate and profile-width values, α and β are estimated to be about $26°$ and $-3°$, respectively.

6 IMPLICATIONS AND ANALYSIS

Despite attempts to define a basic pulsar emission theory (Ruderman & Sutherland 1975; Gil & Sendyk 2000; Hibschmann & Arons 2001; Harding & Muslimov 2002; Wright 2003), there remains very little agreement even in explaining drifting subpulses, an elementary observed feature of so many pulsars. Additional common emission

features that frequently accompany subpulse drift such as mode changing and nulling have received only scant theoretical attention (Jones 1982; Filippenko & Radhakrishnan 1982; Rankin & Wright 2003). Thus, in guiding future theory it is up to observers to establish links and correlations between these phenomena.

Here we take a 'holistic' view of the behaviour of the radio emission of B2303+30. Our hope is that, by considering the observed phenomena of subpulse drift, moding and nulling of this pulsar as aspects of a *single* system, we may learn as much from their interactions as from their separate behaviours.

6.1 The mode system

Let us briefly recap the principal results needed for our synthesis. We have demonstrated in this paper that the emission system of B2303+30 is dominated by two distinctive modes and their interactions. The modes exhibit rapid transitions from one to the other and are usually clearly distinguishable both by their strongly differing intensities and by their altered subpulse behaviour. We are fortunate that the proportion with which the two modes occur is near to even (54 : 46 for B : Q) and that their mean durations ($37P_1$:$31P_1$) are sufficiently short to give us satisfactory statistics within the observing time available. However, the distribution of mode durations (see Fig. 4) does not take the simple Gaussian form that one might reasonably have expected if there were random switching between the modes. First, there are occasional stretches of B mode with long and stable duration well over 100 pulses, which do not belong to the overall pattern. Without these special sequences, the B : Q ratio comes even closer to 50 : 50, suggesting that for some reason the two modes are, for much of the time, in near-equilibrium. Secondly, the excess of mode durations less than 13 pulses appears to create a distortion in the distributions. In Section 3.1 we suggested that this distortion may reflect the presence of numerous short B- and Q-mode sequences in the intervals between the longer and more intense B-mode stretches. It was further suggested that the peak in the Q-mode duration of around 30–40 periods reflects the typical interval length between the strong B-mode sequences.

Nulls strongly interact with the modes system, since we find in this pulsar – for the first time among pulsars – that they overwhelmingly occur in only one of the modes. Nulling is conventionally considered to be a different physical phenomenon to moding. Furthermore, the statistics of null lengths (Fig. 13) are quite different from those of mode lengths (Fig. 4), so that, in this and all other pulsars where they occur, short nulls are more frequent and long nulls rare. This contrasts to the peak of 35–40 pulses in the distribution of B- and Q-mode lengths. However, if we only compare the peak of short-duration modes with the null peaks, then the statistics look far less different. With modes, even more so than with nulls, it is difficult to identify those of short duration. Indeed, it is intrinsically impossible to define anything less than a three-pulse mode! Taking these factors into account, the 'true' distribution of the *short* modes may well have a similar form to that of nulls, and hence may be part of the same system. Again, this is an important clue for our understanding of the system.

Since the B and Q modes have similar durations, and since these are considerably shorter than the length of the observing sessions, we have the opportunity to test whether or not the system is switching modes at random. If the system is not random, then we might expect correlations between the lengths of successive mode appearances: the length of a B-mode sequence may influence the length of the following Q mode (or vice versa), or one B may fix the length of the next B, or the combination of B and Q may form a

non-random sequence, etc. To test whether some unknown physical 'rule' underlies the selection of the modes and the duration of their appearance, we apply a well-known test, developed in the context of chaos theory, to search for order in time series (Takens 1981). It involves using the original time series to create a duplicate time series with a delay of one unit, and generating a sequence of pairs displayed on a two-dimensional graph. If the points on the graph show a tendency to be confined to a particular region, or to follow a particular trajectory, then this is strong evidence that the system has a hidden attractor determined by the physical rule. Using the mode lengths as units, it was possible to experiment with several possible kinds of time series (B length versus next Q length; B length versus next B length; etc.). The typical result was a quasi-cyclic clockwise progression about the mean mode length, but with sufficient anti-clockwise components to give doubt as to whether the result was due to chance. Usually the picture was complicated by the numerous short mode lengths that contribute to the unexpected peak of these in the histogram of Fig. 4.

However, in one observation at 1414 MHz we found a more convincing result: using the length of successive Q modes, a clear cyclic behaviour was revealed (Fig. 16). The S/N of this observation was not as good as in the others and short weak B-mode pulse sequences, which in better observations punctuate the Q mode, were not detected. The histogram of mode lengths for this data set exhibited no excess of short modes. Thus the short mode sequences could somehow be clouding the underlying picture of the B2303+30 system and should be merely seen as elements of a longer-scale quasi-cyclic behaviour. It is important to note that, although plots of *n* versus *n* + 1 are intrinsically cyclic, it would be improbable for a random sequence to produce a plot as circular as the one seen in Fig. 16. No safe conclusion can yet be drawn, but it is important to establish whether the system is changing mode at random. Unlike B0943+10, the mode changes are sufficiently frequent to warrant a multi-hour investigation of this phenomenon.
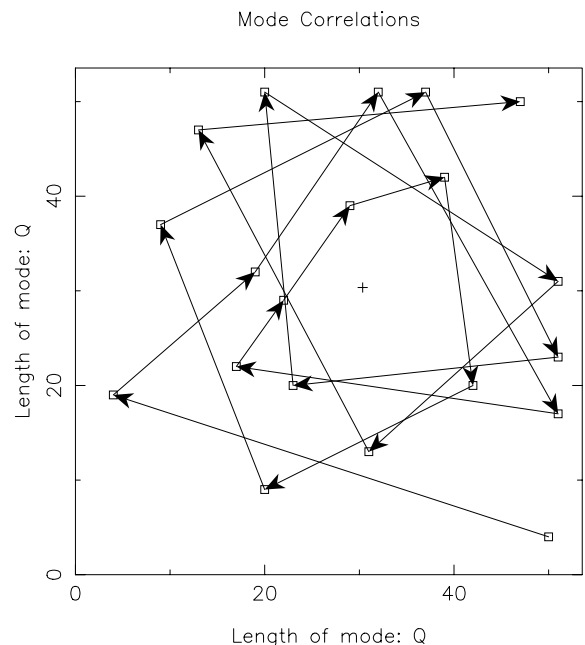

Figure 16. A sequence formed from plotting the length of each Q mode against that of the subsequent Q mode from the 1992 October 18 observation at 1414 MHz. Here a clear quasi-periodic cycle is evident.

6.2 Subpulse modulations

To take our analysis one step deeper, we progress to the subpulse level. The subpulse modulations of each mode, succinctly summarized in the LRF and HRF spectra of Figs 9 and 10, are revealed with great clarity in Fig. 17, which shows three pulse sequences from the same 430-MHz observation. By suppressing the intensity scale so that all but the brightest pulses have the same colour, the two principal phase patterns of the modes are brought to the fore, and we can better study their interaction. Moreover, we can also see an additional mode, most unexpected and often barely discernible, which immediately follows five of the longer B-mode sequences. In this mode, which we call the Q* mode because of its 'conjugate' nature, the drift bands have a reversed slope to those of the Q mode. The new mode, and its position in the sequence of modes, is the key to the model we develop here.
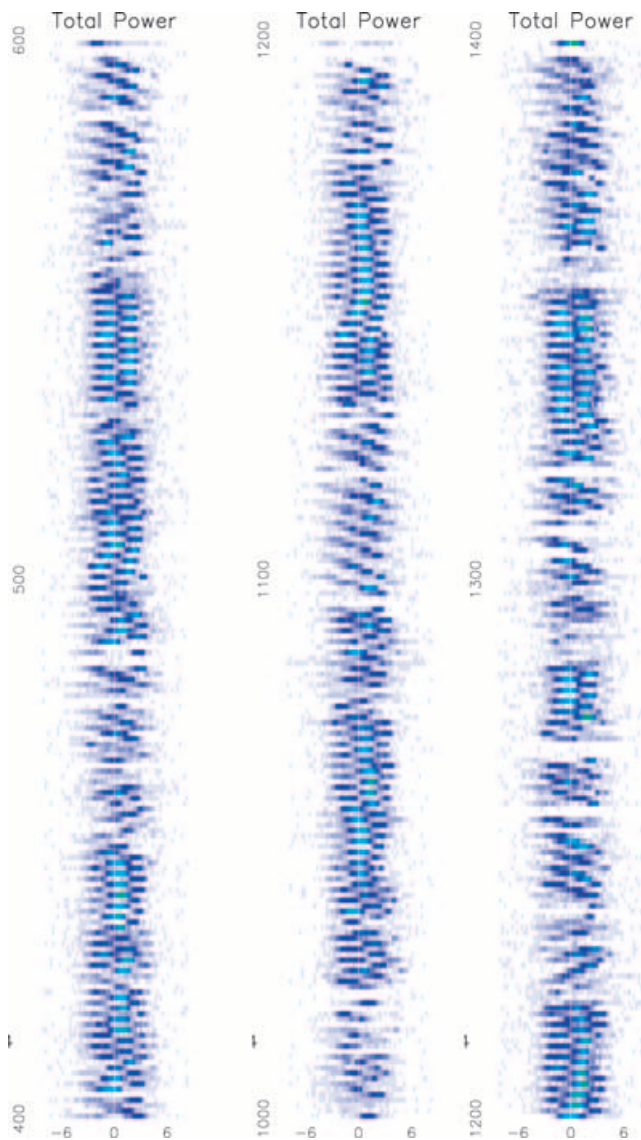

Figure 17. Subpulse sequences at 430 MHz. The colour scaling of Fig. 1 has been amended so that the changing subpulse phase is brought out more clearly. All pulse intensities are shown in shades of blue, with turquoise for the strongest. Note five examples of the unusual Q* mode, all following steady B-mode sequences. These are at pulses 450, 560, 1080, 1220 and 1362.

We begin by considering the properties of the principal modes. Although the P_3 periodicities of both modes are subject to jitter and swing, the fact that one clusters around $2P_1$ and the other $3P_1$ suggests a remarkable harmonic relation, and this is supported by our mode simulation (Fig. 11). Other pulsars (with up to three drift modes) are also known to exhibit 'harmonic' relationships between their discrete P_3 values (e.g. B0031−07, B1918+19, B1944+17, B2319+54, etc.). However, those pulsars have much longer P_3 periodicities (up to about $14P_1$) and their harmonic nature lies in the roughly equal *ratios* of their P_3 values (around $3:2$). B2303+30 not only has two P_3 values with such a ratio, it additionally has a harmonic relation *to the pulsar period itself*. This presents us with what could be a major clue to their physical interpretation, if only it can be comprehended.

A further clue could be the curious fact that B2303+30 belongs to a small but possibly significant group of pulsars with a P_3 very close to $2P_1$. In general, older pulsars (measured by their spin-down rate) are found to have longer P_3 values (seen in fig. 4 of Rankin 1986), a feature that is supported by more recent discoveries of subpulse drift in other pulsars, and it is surprising that there are now seven pulsars of all spin-down ages that have P_3 close to the Nyquist value. The others are B0834+06, B0943+10, B1633+24, B1933+16, B2020+28 and B2310+42. None of these pulsars are known at present to have a second Q-like fluctuation, but, with the exception of B0943+10 (whose Q mode is chaotic; Deshpande & Rankin 2001), little long-term single-pulse study has been undertaken of any of them.

Of course, we cannot be sure that the P_3 values observed in B2303+30 are the true ones. We may be seeing aliases of a faster underlying drift, as has been suggested for the very different pulsar B0826−34 (Gupta et al. 2004). The HRF spectrum for B2303+30 (Fig. 10), powerful though it is in distinguishing the varying periodicities and sense of subpulse drift in apparently confused pulse sequences, is unable to tell us the degree of the underlying aliasing that generates the identified drift. However, a number of arguments, of varying degrees of strength, can be assembled in favour of zero or weak alias for the B mode. First, in the pulsar B0943+10, with which B2303+30 shares many properties, it was conclusively demonstrated (Deshpande & Rankin 2001) that its B-mode on–off emission was not generated by high-order aliasing (in fact it has the pattern of Fig. 18a and $n = 0$ according to the alias ordering system here). Secondly, if the observed P_3 values of both B and Q modes are the result of aliasing to the nth degree, their true P_3 values would be $2/(2n + 1)$ and $3/(3n + 1)$, respectively, and their harmonic ratio to each other and to the rotation period would be weaker and more complex (and, for high n, lost altogether). This would imply that the observed harmonic relations were coincidental. Furthermore, *differential* aliasing between the modes would result in complex transitions (van Leeuwen et al. 2003), yet at least some transitions (see Fig. 3) are observed to occur smoothly. Finally, if the modes were aliased to differing orders, then not only would simple harmonicity be lost, but the modes would have a differing P_2 (through a change in the number of rotating beams observed in a single turn), which is not observed.

Although none of the above arguments is conclusive, we will apply Occam's Razor and make the simplest assumption, namely that the B mode has alias of $n = 0$ or $n = -1$ (i.e. $P_2 = 2$ or -2). We can then determine whether the underlying drift speeds up or slows down between modes. The fact that each of the modes has its characteristic observed P_3 enables us to constrain the possibilities, and Fig. 18 illustrates this point. In both schemes (a) and (b) the direction of the sightline is the same. In (a) (alias $n = 0$) the
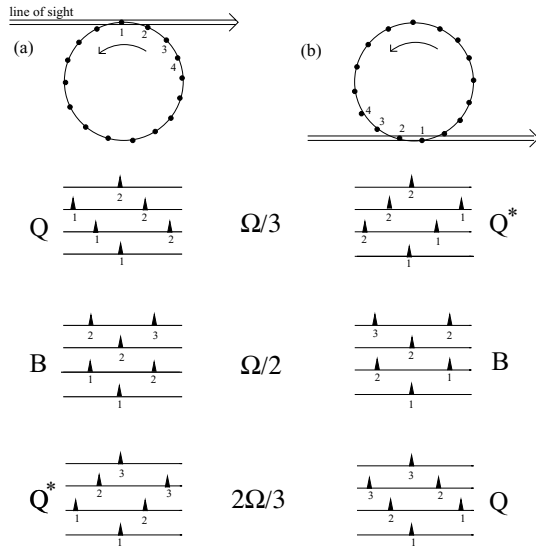
Figure 18. The geometry of B- and Q-subpulse behaviour. The successive sub-beams are represented as a carousel, which rotates at speed Ω, and the panels left and right show the resulting subpulse patterns for varying values of Ω. In case (a) the carousel rotates counter to the sense of our sightline passage, and in (b) in the same sense, implying that (a) represents an observer traverse between the magnetic and rotation axes, and (b) outside both. The rarely observed Q* mode has the same periodicity as mode Q but drifts in the opposite sense. Thus Q* is the aliased mode in (a) and Q in (b). In the text we argue that (a) is the more likely system for B2303+30 on observational grounds. The rotation rate Ω corresponds to the rate at which sub-beam 2 would move to the position of sub-beam 1 within one pulse period.

underlying drift is counter to this direction and in (b) (alias $n = -1$) it has the same sense. In the B-mode drift, assumed for simplicity to have an observed P_3 of exactly $2P_1$, the on–off system appears in both cases, but in (a) with the central subpulse repeating on the leading side as the drift progresses, and in (b) on the trailing side. If a secondary drift towards the trailing edge is observed (e.g. pulses 60–90 in Fig. 1), this corresponds to an acceleration in case (a) (i.e. *true* $P_3 < 2P_1$) and a deceleration in case (b) (*true* $P_3 > 2P_1$). Note that this argument does not actually depend on the beams forming the carousels shown in Fig. 18, nor on the number of such beams: it merely concerns the sequence in which the beams are presented to the observer. However, if the beams do take the form of a carousel, then the line-of-sight traverse is interior in (a) and exterior in (b) to the angle between the magnetic and rotation axes, otherwise the net rotation of the carousel would exceed the rotation of the star.

In Section 5 we presented tentative observational arguments for believing that our sightline passes between the rotational axis and the magnetic axis (an inner traverse). These arguments were quite independent of the discussion in this section and, if true, support our preference for the subpulse system of Fig. 18(a). With this choice, we not only conclude that the elegant observed harmonic ratios correspond to true harmonics, but we find that our view of the emission cone of B2303+30 follows an inner traverse in essentially the same manner as for B0943+10, and the subpulses of both pulsars are presented to us in the same sequence without alias.

6.3 Mode transitions

With the help of Fig. 18 we can examine how the B-mode system with $P_3 \simeq 2P_1$ migrates to a Q mode with $P_3 \simeq 3P_1$ and the drift proceeding from trailing to leading edge (assuming no change in

subpulse spacing). The transition will be different in cases (a) and (b). The simplest ($n = 1$) migration for (a) would be for the movement of the beams to slow to two-thirds from their B-mode speed (as shown). The subpulse arrangement would then imply that in the Q mode each sub-beam was tracked across the drift band (the uppermost drift panel of Fig. 18a). For the case (b) (i.e. n negative) the simplest ($n = -1$) migration would be a small acceleration to four-thirds of its B drift rate, again leading to Q drift bands with $P_3 = 3P_1$, but aliased so that successive subpulses in a single band are successive sub-beams (the lowest drift panel Fig. 18b). In either case, solutions with higher-order alias are of course possible: for example, the beams could accelerate from B to $(n - \frac{1}{3})$ times their original speed ($|n| > 1$), and thereby create an aliased Q drift with P_3 apparently $3P_1$. We argue against this above, but here we can be more specific: More highly aliased transitions would require the rotation to more than double and accelerate through a Nyquist boundary, resulting in an apparently near-stationary drift. Careful inspection of the pulse sequences shows no convincing evidence of such drift patterns, and no low-frequency features between 0.1 and 0.2 c/P_1 appear in the fluctuation spectra of Figs 9 and 10. It is theoretically possible to contrive the observed smooth transitions in a highly aliased system if no Nyquist boundary needs to be crossed. However, in the absence of any evidence for such aliasing, we assume that the transition from B to Q drift is the result of a change in the drift rate by either $\pm\frac{1}{3}$ of the B-mode drift rate.

In many cases the observed transitions from B drift to a regular Q drift and back are far from smooth. In Fig. 1 we can see that nulls or apparently disordered pulses often intervene. However, there is a marked difference between B $\rightarrow$ Q and Q $\rightarrow$ B transitions, as can be seen in the phase-enhanced sequences of Fig. 17. In the former case, the B mode, shortly before the transition, is relatively steady and close to its $P_3 \simeq 2P_1$ state. Only in the B mode's last few pulses, if at all, does its aliased drift begin to strengthen towards the leading edge. This is then followed either by some disorder or by nulls or, in many cases, by drift $P_3 \simeq 3P_1$ *in the opposite sense* to the standard Q drift, designated as Q* in Fig. 18. In the Q $\rightarrow$ B case, as the B mode recommences, there is often a strong drift from the trailing edge, which mirrors the concluding behaviour of the B mode in its transition to Q, but here this effect is usually stronger and more marked, and continues with damped oscillating drift patterns well into the B mode. Furthermore, no Q* drift is ever seen before a switch to the B mode. This clear distinction between the two kinds of transition gives the subpulse sequence a 'time arrow'.

It is striking and unexpected that when steady B-mode drift begins the process that ultimately leads to the Q-mode drift, it first suddenly shifts its drift in a sense opposite to what we have identified as Q-mode drift. This can be clearly seen after pulse 450 in the first sequence of Fig. 17, and at four other positions in these sequences. In terms of the carousel picture of Fig. 18(a), this requires that the sub-beams accelerate from the configuration B away from Q towards the subpulse pattern Q*. In many cases this is exactly what is observed, although the acceleration is not always sufficient to achieve a clear Q* pattern.

6.4 The B2303+30 system and 'events'

We are now in a position to interpret the constantly changing drift patterns in terms of varying sub-beam rotation rates on the basis of the model in Fig. 18. The changes from a steady B mode sequence to Q are sometimes very sudden, and we designate these as 'events', without prejudice to their underlying physical cause [this convenient nomenclature was introduced by Lyne & Ashworth (1983)
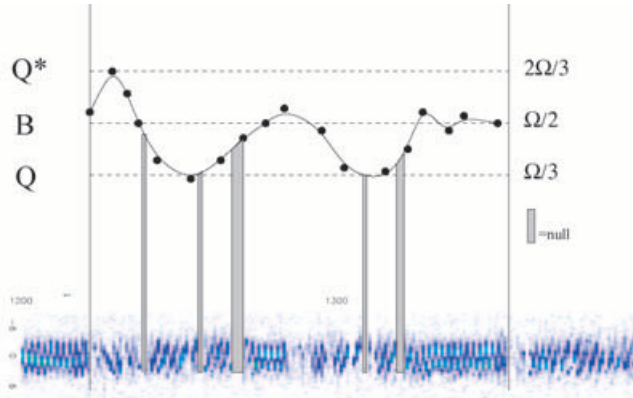
Figure 19. The varying drift rate following an 'event' derived from the subpulse sequence in the right-hand panel of Fig. 17 and interpreted as sub-beam rotation in terms of the scheme in Fig. 18(a). Note the sudden sharp increase in subpulse drift towards the Q* drift rate followed by a slow relaxation through successive B-mode and Q-mode interludes, before returning to a sustained and weakly oscillating B mode. There is a suggestion that nulls may be associated with rapid drift rate changes.

in connection with the nulls of B0809+74, and also by Janssen & van (2004) for B0818−13]. Other changes are more gradual, and appear to be part of an on-going process. As an illustration of our technique, in Fig. 19 we have analysed a pulse sequence extracted from the right-hand column of Fig. 17 and interpreted by means of Fig. 18 as a single cycle. The main features are as follows:

(i) Starting in a steady B-mode sequence there is little hint of the impending mode change, just occasionally a sudden shift in the aliased secondary drift towards the leading edge, before the B-mode intensity is lost. In other sequences this 'warning' shift towards the end of B can be more gradual.

(ii) The Q mode commences as a single sudden event, causing an accelerated drift to the leading edge and a weakening in intensity, sometimes apparently provoking a null sequence and/or an excursion to the Q*-mode drift rate. Here the effect is unusually powerful. According to the subpulse schemes in Fig. 18 this implies that the subpulses have either (a) accelerated or (b) decelerated *away* from the rotation rate corresponding to Q-mode drift.

(iii) Having achieved a peak in the Q* sense, the drift rate begins to fall back, passing rapidly through the rate associated with B and moving towards a typical Q-mode rate. Throughout the entire cycle, nulls are often noted at points where rapid change in drift can be inferred.

(iv) Whether or not the Q drift rate is reached, the drift rate continues to oscillate with gradually reducing amplitudes around the mean B-mode value.

(v) Whenever Q-mode drift is achieved (e.g. pulses 1242–1265 and 1300–1320), the emission is relatively stable and bright, albeit sometimes interspersed with nulls.

(vi) Finally the B mode is re-established in the form of a weak damped wave in the drift rate around the B-mode value, which gradually peters out until the next event. These closing B-mode sequences are often approached by subpulse motion from the trailing edge (see pulse 1325), indicating that the drift rate has made a further oscillation towards Q* and not smoothly returned from the Q-drift sequence.

The sequence (i) to (vi) exemplifies the cyclic nature of this pulsar's behaviour. Although here at its most complex, it is possible to

trace the swings in drift rate through 133 pulses. Other cycles are shorter and may sometimes consist of just a single shallow oscillation, but all share the property of an event followed by a gradual relaxation to the B mode. The intensity of the events, measured by the amplitude of the initial perturbation in the drift rate towards (but only rarely achieving) the Q* pattern, can vary considerably. It is difficult to assess whether events are occurring at random in the pulse sequence (see Section 6.1), but the evidence of Fig. 17 and numerous other sequences suggest that the B mode is the underlying asymptotic steady state, which, once achieved, triggers a fresh event in a never-ending feedback system.

As a cycle progresses we see a sequence of short B and Q stretches and short nulls generated by the rapid oscillation in the sub-beam rotation rate. It is this which generates the coupled distributions of short B, Q and null sequences referred to in Section 6.1. Longer B sequences (peaking at $37P_1$ in Fig. 4) represent relatively stable B conditions leading up to an event. Longer Q sequences (peak $31P_1$) apply to the apparently confused sequences following an event, where, in the underlying cycle, the B drift rate is never sustained over sufficient time or intensity to be identified.

Thus we may conjecture that the emission of this pulsar is governed by a series of 'events': unspecified physical impulses that suddenly change the drift rate, and from which the emission takes many rotation periods to recover. They appear to be triggered in the B mode by the very stability of its subpulse pattern, suggesting that the B mode is the pulsar's asymptotic equilibrium state upon which the events act. Following an event, the average relaxation time will be approximately the sum of the average durations of the B and Q modes in their longer manifestations (i.e. the peaks on the broader mode length distributions in Fig. 4). This sum is around 80 pulses and generates the low-frequency feature in Figs 9 and 10.

7 THE MAGNETOSPHERE OF B2303+30

7.1 Comparison with B0943+10

As pointed out earlier, B2303+30 is one of seven pulsars that exhibit an on–off intensity variation with P_3 around $2P_1$. The seven have apparently little in common in their basic parameters of rotation period, inferred magnetic field strength and spin-down age, so the effect may be a coincidence, but the wide range of the last of these parameters (from B0834+06 with a timing age of 3 Myr up to B1633+24 with 65 Myr) is interesting since it defies the empirical rule of most pulsars with subpulse drift (shown in fig. 4 of Rankin 1986) that P_3 increases with age.

The pulsar from this group with parameters closest to B2303+30 is B0943+10, and this fact was initially the impulse for the present investigations. Many detailed investigations of B0943+10 have been published in recent years (e.g. Deshpande & Rankin 2001), its attraction being its precise P_3 modulation (close to $1.87P_1$) combined with a regular longer-term modulation, which have enabled these authors to establish uniquely that the pulsar fits a model of 20 emission columns circulating around the star's magnetic pole.

Both B0943+10 and B2303+30 have relatively long periods (1.1 s versus 1.6 s – and hence similar light-cylinder radii). They have comparable timing ages (5 Myr versus 8.6 Myr) and they have near-identical inferred surface magnetic fields (2×10^{12} G), so that their light-cylinder magnetic fields only differ by a factor of <3, and the magnetospheric electric field, which governs the drift rate (Ruderman & Sutherland 1975; Gil & Sendyk 2000; Wright 2003), will be of the same order in both pulsars. However, there are fundamental differences. In the B mode of B2303+30 there is a clear

'jitter' in the P_3 modulation, sometimes sudden and sometimes gradual, but in any case within about 40 periods, which makes it impossible to uncover any circulatory modulations that the emission beams may possess and hence prevents us from determining the direction of the beams' rotation with respect to the observer. Curiously, our derived figure for the average duration of the B mode in B2303+30 ($\simeq 37 P_1$) is virtually identical to the circulation time given for the sub-beam carousel in B0943+10 ($37.35 P_1$). In any case the frequent 'events' in B2303+30, which give rise to fascinating interplay between B and Q modes, prevent the asymptotic B mode from being maintained for any great length of time.

The greatest contrast between the two pulsars lies in the behaviour of their respective Q modes. That of B0943+10 is undoubtedly highly chaotic with no periodic features reliably detected so far (although, intriguingly, some remnant memory of the circulation timescale similar to the B mode does seem to persist). In B2303+30 we have demonstrated beyond doubt that a clear and unambiguous drift with a periodicity of around $3 P_1$ frequently occurs in its Q mode. Furthermore, nulls are found to be common in this mode (Fig. 12), and none have been detected in either mode of B0943+10. The Q mode of B2303+30 is marked by a considerable fall in intensity (Fig. 8). This is also true of the Q mode of B0943+10, but there can be sudden powerful pulses and in general a greater 'spikiness' of emission. The reason for their differences might lie in their differing angles of inclination [in the model of Wright (2003) this is a critical factor in determining the characteristics of subpulse drift] or in the relative sizes of their emission cones. The angle for B0943+10 has been reliably fitted to about 15° (Deshpande & Rankin 2001) on an outer cone. However, in Section 5, we argue, on the basis of the frequency dependence of its profile, that B2303+30 is at an angle of 26° and that we are seeing an inner cone. Nevertheless, our sightline traverses both pulsars on an inner passage between the magnetic pole and the rotation axis.

Relatively little is known about the relative occurrence of the two modes in B0943+10 since both modes typically last several hours, but it is likely to be more weighted towards B than the figure (B : Q = 54 : 46) obtained here for B2303+30 (Rankin & Suleymanova 2005). One interesting point of similarity is the observation in B0943+10 that the B mode anticipates its mode change to Q by slow changes in its drift rate (Suleymanova & Izvekova 1989). This can be seen as a more gradual version of the slight shift in the B drift pattern to the leading edge immediately before an event [see item (i) in the list in Section 6.4]. On the whole, one has the impression that B2303+30 is a speeded-up, more impatient, version of B0943+10: the modes switch much more frequently by a factor of at least 250, and the drift rates vary by a far greater factor.

7.2 Emission models

Gil & Sendyk (2000) have applied their modified form of the Ruderman & Sutherland (1975) polar cap model to B2303+30. Their fit was based on two 'submodes' of the B mode, with P_3 just under $2 P_1$, i.e. scheme (a) in Fig. 18. They fitted a ring of 12 sparks on an outer cone with an interior traverse on an assumed axis inclination of 50°. Our considerations in Section 5 put the lower figure of 26° on the inclination and suggest an inner cone, so their model may need refitting to check these changed parameters. The discovery here of a steady Q-mode drift substantially different from the B-mode drift will, in the context of a polar cap model, require the surface electric field to make adjustments of up to 50 per cent in a very short time (less than one rotation period) and this is difficult to accommodate. However a revised version of the theory (Gil,

Melikidze & Geppert 2003), wherein much of the electric field is screened close to the surface, may counter this objection.

A magnetosphere-wide feedback model can be constructed for the B-mode drift along the lines of the published fit to the B0943+10 drift (Wright 2003). This model regards the radio emission from close to the surface to be driven by particle infalls from the outer magnetosphere, particularly from a weakly pair-creating outer gap. The pattern of the subpulse drift in this model is highly dependent on the inclination angle, since it is this which determines the location of the outer gap, and predicts that stable slow drifting and slow long-term cycles are more likely in nearly aligned pulsars. More inclined pulsars will experience faster drift and more frequent moding because of the greater variations in the electric fields in the less stable magnetospheres of such pulsars (Rankin & Wright 2003). In B2303+30 the mode changes are relatively frequent, so an inclination in the 20°–30° range might be expected. In this model, a mode change might correspond to a shift in the location of the outer pair-creation site along the zero-charge surface, thereby changing the time-scale of the feedback system.

What is the nature of the 'events' that we have identified here as the instigators of the mode changes? In B1237+25, a highly inclined pulsar ($\alpha \simeq 53°$), where we have the advantage of a sightline passage directly over the magnetic pole, the mode transition from an ordered to a disordered mode is always accompanied by activity in the core region of the profile close to the magnetic pole. These polar 'eruptions' appear also to interfere with the normal mode on a quasi-periodic time-scale of around $40 P_1$ (Hankins & Wright 1980; Srostlik & Rankin, in preparation). In B2303+30 our sightline cuts only the fringe of the emission cone, so perhaps the sudden 'events' are due to unseen activity along the pulsar magnetic axis. On the other hand, the fitted drift rate curve in Fig. 19 closely resembles those found in studies of non-linear damping of the potential in electrical systems (e.g. the van der Pol 1927 equation), where sudden changes in potential are just chaotic fluctuations in a completely deterministic system, and these require no *Deus ex machina*.

Neither model seems able to explain the harmonic relation between the observed $P_3 = 2 P_1$ and $P_3 = 3 P_1$ subpulse fluctuations. Noting that dipole geometry is built on the ratio 2 : 3 (e.g. the inner and outer radial limits of the 'null' or zero net-charge line are in the ratio of $(\frac{2}{3})^{3/2}$), we can speculate that the harmonics might correspond to 'eigensolutions' in the configuration of the magnetosphere at large.

8 CONCLUSIONS

We list the principle conclusions of this paper below:

(1) B2303+30 has two modes of emission, B and Q, the former being more intense and more organized. The Q-mode profiles are slightly wider in shape than those of the B mode at all frequencies, and the profiles of both modes are single-peaked and significantly asymmetric. This asymmetry is also present in longitudinal cross-correlations and fluctuation spectra.

(2) Each of the modes exhibits a characteristic subpulse behaviour. The B mode has an on–off pattern with a fluctuation frequency close to $2 P_1$, sometimes steady and sometimes weakly modulated. The Q mode is more irregular, but often exhibits distinctive fluctuations with P_3 close to $3 P_1$. There is no evidence of change in P_2, the subpulse spacing, from one mode to the other. Thus an apparent harmonic relation exists between the drift rates of the modes and, quite remarkably, each mode is harmonically related to the pulsar rotation period.

(3) Nulls occur predominantly, possibly exclusively, within the Q-mode sequences, often close to the start or ending of the Q mode. This is the first pulsar in which nulls have been shown to be confined to a particular emission mode. There is evidence that nulls occur when the subpulse drift rate is undergoing rapid change.

(4) All the observed subpulse features are closely knit into a single emission system. The system consists of a series of cycles, each begun by an 'event', occurring when the B mode is relatively stable. This results in rapid drift rate changes, which we identify as the Q mode. Surprisingly, the event's initial effect, whether great or small, is generally counter to the variation required to bring about the Q-mode drift, and, when strong, achieves a subpulse pattern with $P_3 \simeq 3P_1$, as in the usual Q drift, but with the sense of drift reversed (this we call Q* drift).

(5) The drift rate then gradually relaxes back asymptotically to the steady B-mode drift rate, often in a roughly oscillatory manner over many pulses. The total relaxation period averages 80 pulses, and depends on the intensity of the event. Swings in the drift rate lead to short alternating stretches of Q*, B and Q drift, interrupted by nulls that frequently occur when the underlying sub-beam rotation is varying rapidly. Conversely, bright pulse sequences of either B or Q mode are correlated with slow variations in drift.

(6) The changing drift rates can be modelled as damped oscillations in the sub-beam circulation rate. The circulation rate is found never to vary more than $\pm\frac{1}{3}$ from that of the B-mode. In the simplest case (our preferred solution) the sub-beam rotation is counter to the sense of the observer's sightline in an *internal* traverse (Fig. 18a). This implies that the Q* drift is aliased, but B and Q are not: the change from B- to Q-mode drift slows the sub-beam rotation to two-thirds of its B rate, whereas directly after 'events' the circulation rate speeds up (by one-third in the case of Q*). Then the *true* B-mode P_3 is just below $2P_1$, as in the case of B0943+10, and the mean *true* P_3 for Q is exactly $3P_1$.

(7) The geometry of the circulation model is independently supported by the evidence from the frequency dependence of the pulsar's profile. This suggests that B2303+30 is inclined at an angle of 26° and that our sightline makes an interior traverse of an inner cone.

(8) The B mode can be seen as the pulsar's asymptotic steady state, which nevertheless cannot be sustained for long without triggering an event. There is evidence (Fig. 16) that the occurrence and intensity of the events are not randomly distributed, and may themselves have a quasi-cyclic behaviour.

REFERENCES

Backer D. C., 1973, ApJ, 182, 245
Deshpande A., Rankin J. M., 1999, ApJ, 524, 1008
Deshpande A., Rankin J. M., 2001, MNRAS, 322, 438
Filippenko A. V., Radhakrishnan V., 1982, ApJ, 263, 828
Gil J. A., Sendyk M., 2000, ApJ, 541, 351
Gil J. A., Hankins T. H., Nowakowski L., 1992, in Hankins T. H., Rankin J. M., Gil J., eds, IAU Colloq. 128, The Magnetospheric Structure and Emission Mechanisms of Radio Pulsars. Pedagogical Univ. Press, Zielona Góra, Poland, p. 278
Gil J. A., Melikidze G. I., Geppert U., 2003, A&A, 407, 315
Gupta Y., Gil J., Kijak J., Sendyk M., 2004, A&A, 426, 229
Hankins T. H., Rankin J. M., 2005, ApJS, submitted
Hankins T. H., Wolszczan A., 1987, ApJ, 318, 410
Hankins T. H., Wright G. A. E., 1980, Nat, 288, 681
Harding A., Muslimov A., 2002, ApJ, 568, 864
Hibschmann J., Arons J., 2001, ApJ, 560, 871
Janssen G., van Leeuwen J., 2004, A&A, 425, 255
Jones P. B., 1982, MNRAS, 200, 1081
Lang K. R., 1969, ApJ, 158, 175
Lyne A. G., Ashworth M., 1983, MNRAS, 204, 519
Lyne A. G., Manchester R. N., 1988, MNRAS, 234, 477
Malofeev V. M., Izvekova V. A., Shitov Yu. P., 1989, AZh, 66, 345
Oster L., Hilton D. A., Sieber W., 1977, A&A, 57, 323
Ramachandran R., Rankin J. M., Stappers B. W., Kouwenhoven M. L. A., van Leeuwen A. G. J., 2002, A&A, 381, 993
Ramachandran R., Backer D. C., Rankin J. M., Weisberg J. M., Devine K. E., 2004, ApJ, 606, 1167
Rankin J. M., 1983, ApJ, 274, 333
Rankin J. M., 1986, ApJ, 301, 901
Rankin J. M., 1990, ApJ, 352, 247
Rankin J. M., 1993a, ApJ, 405, 285
Rankin J. M., 1993b, ApJS, 85, 145
Rankin J. M., Ramachandran R., 2003, ApJ, 590, 411
Rankin J. M., Suleymanova S. A., 2005, AAS Meeting 205, No. 111.09
Rankin J. M., Wright G. A. E., 2003, A&AR, 12, 43
Rankin J. M., Campbell D. B., Backer D. C., 1974, ApJ, 188, 609
Ruderman M. A., Sutherland P. G., 1975, ApJ, 196, 51
Sieber W., Oster L., 1975, A&A, 38, 325
Suleymanova S. A., Izvekova V. A., 1996, Astr. Lett., 22, 810
Suleymanova S. A., Izvekova V. A., Rankin J. M., Rathnasree N., 1998, JA&A, 19, 1
Takens F., 1981, in Rand D. A., Young L.-S., eds, Lecture Notes Maths, Vol. 898, Dynamical Systems and Turbulence. Springer, New York, p. 366
Taylor J. H., Huguenin G. R., 1971, ApJ, 167, 273
van der Pol B., 1927, Phil. Mag., 3, 65
van Leeuwen A. G. J., Stappers B. W., Ramachandran R., Rankin J. M., 2003, A&A, 399, 223
Wolszczan A., 1980, A&A, 86, 7
Wright G. A. E., 2003, MNRAS, 344, 1041
Wright G. A. E., Fowler L. A., 1981a, A&A, 101, 356
Wright G. A. E., Fowler L. A., 1981b, in Sieber W., Wielebinski R., eds, Proc. IAU Symp. 95, Pulsars. Reidel, Dordrecht, p. 221

This paper has been typeset from a TEX/LATEX file prepared by the author.